CONTROLLING AND MANIPULATING THE TOPOLOGICAL SPIN OF MAJORANAS

by
EMRE DUMAN

Submitted to the Graduate School of Engineering and Natural Sciences
in partial fulfilment of
the requirements for the degree of Master of Science

Sabancı University
July 2025

TOPOLOGICAL SPIN OF MAJORANAS

Approved by:

Prof. İNANÇ ADAGİDELİ .....
(Thesis Supervisor)

Prof. ZAFER GEDİK .....

Prof. AHMET LEVENT SUBAŞI .....

Date of Approval: July 17, 2025

ABSTRACT

CONTROLLING AND MEASURING THE TOPOLOGICAL SPIN OF MAJORANAS

EMRE DUMAN

Physics, M.Sc. Thesis, July 2025

Thesis Supervisor: Prof. İnanç Adagideli

Keywords: Majorana-zero-mode, topological-spin, Fermi-sea, topological-insulator

Majorana zero modes (MZMs) have attracted interest both for their fundamental physics and for their potential technological applications. While the non-Abelian phase associated with a braiding operation is widely recognized, the accompanying Abelian phase of $-\pi/4$ does not enjoy the same level of recognition. The non-Abelian exchange statistics of Majorana zero modes make them suitable for potential applications in fault-tolerant quantum computation and topological quantum computing For this reason, finding physical platforms capable of realizing these exotic quasiparticles in condensed matter systems is an active area of research. In this thesis, we focus on the Abelian exchange phase of Majorana zero modes. We examined this phase in two well-known models of topological superconductors: the Fu-Kane model and hybrid structures of superconductor / quantum anomalous Hall (QAH) insulators. We demonstrated that this phase originates from an Aharonov-Casher phase generated by a superconducting vortex encircling a charge of $-e/4$ associated with the Fermi sea. Next, in two-dimensional (2D) systems, we showed that the fractional charge and the Majorana zero mode are co-located in the core of the superconducting vortex, whereas in three-dimensional (3D) systems, the fractional charge and the Majorana mode can be spatially separated. In doing so, we designed a heterostructure system that enables the manipulation of both the Abelian and non-Abelian contributions of Majoranas. Finally, we proposed a superconducting vortex interference experiment capable of directly detecting the effects of the isolated Abelian exchange phase discussed here.

ÖZET

MAJORANALARIN TOPOLOJİK SPİNİNİN KONTROLÜ VE ÖLÇÜMÜ

EMRE DUMAN

Fizik Yüksek Lisans Tezi, Temmuz2025

Tez Danışmanı: Prof. Dr. İnanç Adagideli

Anahtar Kelimeler: Majorana-sıfır-modu, topolojik-spin, Fermi-denizi, topolojik-yalıtkanlar

Majorana sıfır-modları (MZM'ler) hem temel fizik hem de teknolojik uygulama potansiyeli açısından ilgi görmektedir. Bir değişim (örgü) işlemiyle ilişkin Abelyen olmayan faz yaygın bir şekilde tanınırken, buna eşlik eden $-\pi/4$ Abelyen faz aynı tanınırlılığa sahip değildir. Majorana sıfır modlarının Abelyen olmayan değişim istatistikleri, onları hata toleranslı ve topolojik kuantum hesaplama alanlarındaki potansiyel uygulamaları için uygun yapmaktadır. Bu sebeple, yoğun madde sistemlerinde bu egzotik kuazi parçacıkları gerçekleştirebilecek fiziksel platformların bulunması aktif bir araştırma konusudur. Bu çalışmada Majorana sıfır modlarının Abelyen değişim fazına odaklandık. Topolojik süperiletkenlerin özellikle iki iyi bilinen modeli olan Fu-Kane modeli ve süperiletken/kuantum anormal Hall (QAH) yalıtkanı hibrit yapılarında bu fazı inceledik. Bu fazın, Fermi denizi ile ilişkili olan $-e/4$'lük bir yükün etrafında dolanan bir süperiletken girdabın oluşturduğu Aharonov-Casher fazından kaynaklandığını gösterdik. Sonra, iki boyutlu (2D) sistemlerde, kesirli yükün Majorana sıfır modu ile birlikte süperiletken girdap çekirdeğinde ortak konumlandığı, fakat üç boyutlu (3D) sistemlerde, kesirli yük ve Majorana modunun ayrıştırılabilineceğini gösterdik. Böylece Majoranaların Abelyen ve Abelyen olmayan katkılarının manipüle edilmesinin yolunu açan bir hetero-sistem tasarımladık. Son olarak, buradaki izole edilmiş Abelyen değişim fazının etkilerini doğrudan tespit edebilecek bir süperiletken girdap girişim deneyi önerdik.

ACKNOWLEDGEMENTS

I want to thank my parents for supporting me throughout my physics journey, and my sister for ensuring, courtesy of her idiosyncratic persuasion techniques, that they did so.

I want to thank Dr. Ahmet Mert Bozkurt and Stijn de Witt for their guidance and for the endless patience and understanding they have shown throughout my less than brilliant moments. I also want to thank Professor Alexander Brinkman and his group at ICE for warmly welcoming me in their team.

I would like to thank my thesis jury members, Professor Zafer Gedik and Professor Ahmet Levent Subaşı, for their constructive criticism and valuable feedback.

Last but certainly not least, I am deeply grateful to my supervisor, Professor İnanç Adagideli, for his guidance throughout my formative years as a physicist. His generosity, insight , and patience during my MSc journey have been invaluable, and have enabled me to complete this thesis to my satisfaction.

Dedicated to the memory of Kırpık,
beloved father and friend to the poor and the homeless.

TABLE OF CONTENTS

LIST OF TABLES

LIST OF FIGURES

1. INTRODUCTION

The topological spin of a particle determines the phase it acquires due to an exchange operation. Exchange of Majorana zero modes (MZMs) implements unitary gates for topological quantum computing; therefore, the topological spin of MZMs is a valuable control knob. In this thesis, based on original work[1], we demonstrate that the topological spin of Majoranas in superconducting vortices is related to a fractional Fermi-sea charge. In addition to the charge associated with the topological spin, superconducting vortices in topological insulators might bind a charge due to the Witten effect. It is possible to fuse these two contributions to tune the topological spin of the composed particle. Furthermore, we propose that the topological spin might be observed through its connection to the fractional charge.

This thesis is organized as follows:

In chapter 2 we focus on the topological spin of Majorana and its manipulation. In section 2.1, we define the Witten effect, and show that an $e/4$ fractional charge is bound to vortices in topological superconductors due to it. We then establish the equivalence between the topological spin and the Fermi-sea charge in section 2.2. Here, a distinction appears: In bona-fide 2D systems, the two contributions necessarily fuse, whereas in 3D systems, the two contributions can be separated and brought together at will. This distinction is examined in section 2.3. Next, Section 2.4 presents the numerical simulation methods used to analyse the phenomena mentioned above, including constructing the BCS ground state in Section 2.4.1.

In chapter 3, we focus on the measurable consequences of the topological spin. We present a proposal for a vortex interference experiment that demonstrates that the contribution of the fractional charge is observable. We derive the circuit QED Hamiltonian describing our experimental setup in section 3.1, and show the mapping of the circuit QED Hamiltonian to a tight-binding model in section 3.2.

We provide section summaries where meaningful, and a conclusion in chapter 4.

[1] Available as a preprint in (de Wit, Duman, Bozkurt, Brinkman & Adagideli, 2025) at the time of submitting this thesis.

2. THE TOPOLOGICAL SPIN OF MAJORANAS

The existence of Majorana Fermions as an elementary particle is an unresolved issue; however, it is predicted that they emerge as low-energy quasi-particle excitations in condensed matter systems. MZMs[1], exhibit non-Abelian exchange statistics which enable quantum computational gates (Beenakker, 2020; Castagnoli & Rasetti, 1993; Lahtinen & Pachos, 2017; Nayak, Simon, Stern, Freedman & Das Sarma, 2008) to be implemented in a fault-tolerant, topologically protected way (Kitaev, 2003). There is an ongoing search for condensed matter systems that realize MZMs (Beenakker, 2013; Lutchyn, Bakkers, Kouwenhoven, Krogstrup, Marcus & Oreg, 2018; Yazdani, von Oppen, Halperin & Yacoby, 2023). In this study, we focus on MZMs bound to vortices: Majorana vortices were first identified in p-wave superconductors (Caroli, De Gennes & Matricon, 1964; Jackiw & Rossi, 1981), where their exchange statistics were shown to resemble those of non-Abelian quasiparticle excitations in quantum Hall systems (Ivanov, 2001; Read & Green, 2000). Subsequently, MZMs were also predicted in superconductor-topological insulator (SC–TI) proximity structures (Cook & Franz, 2011; Fu & Kane, 2008).

In this Chapter, we explore the fractional charge of vortex-bound Majorana modes in TI-SC systems, as seen in Fig 2.1. First, in Section 2.1, we employ a topological Lagrangian term to examine the fractional charge induced on a topological insulator by vortex flux from a type-II superconductor, called the Witten effect. Then, we make the connection between topological spin and the fractional charge in Section 2.2. We find in Section 2.3 that the Witten effect charge and the fractional charge due to the topological spin fuse, and co-localize in 2D systems; in 3D systems, on the other hand, we can tune the gaps of the system, the magnetization strength β and superconducting pair potential strength Δ_0, to move the MZM and the Witten effect charge on opposite ends of the system. Finally, in Section 2.4, we show how to calculate the charge, and Berry connection, using tight-binding models.

[1] In a superconductor, the fundamental excitations are Bogoliubov quasiparticles, described by operators that are linear combinations of fermionic creation and annihilation operators, mixing particle and hole components. A Majorana zero mode (MZM) is a special case: a Bogoluibov quasiparticle with exactly zero energy, whose operator is self-conjugate; and hence, two MZMs are required to form a fermion. MZMs carry no net charge, and often exhibit topological protection against local perturbations.

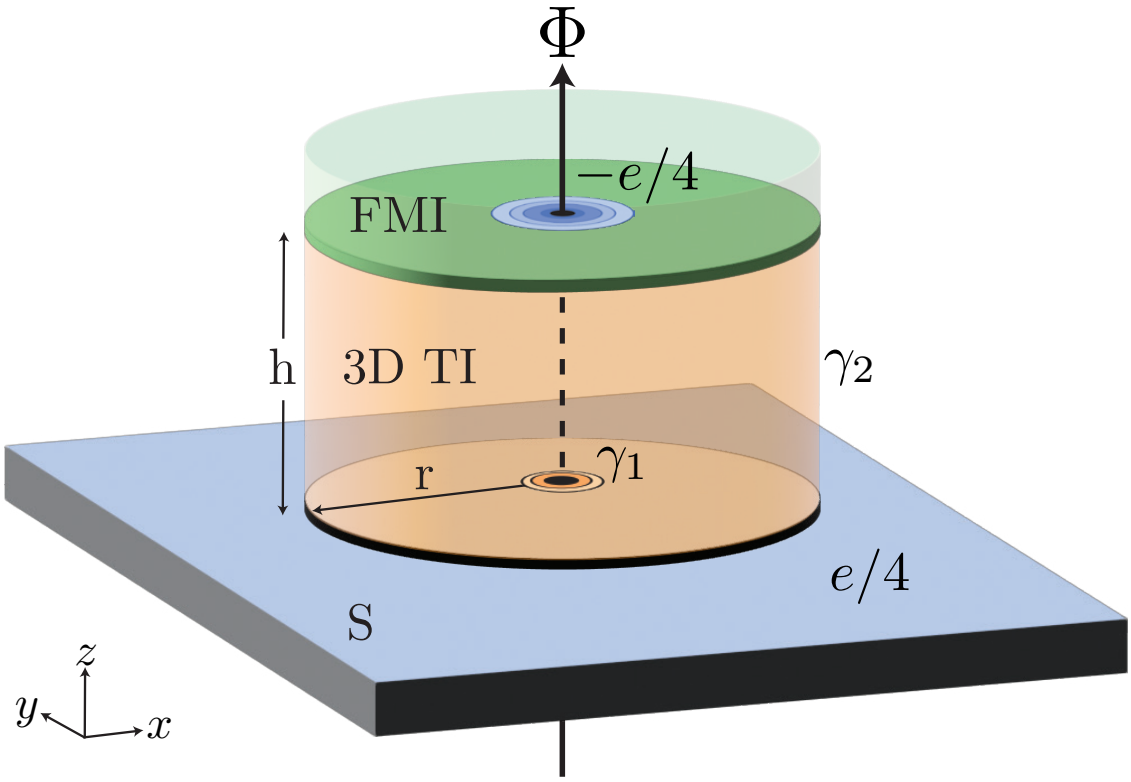

Figure 2.1 S/3D TI/FMI heterostructure. A 3D topological insulator (TI) cylinder with radius r and height h is coupled to an s-wave superconductor (S) below and a ferromagnetic insulator (FMI) above. A vortex induces a magnetic gap $\beta(z)$ and pairing potential $\Delta_0(z)$, binding a fractional charge $-e/4$ at the TI/FMI interface. Majorana zero modes (MZMs) localize on opposite surfaces: γ_1 at the S/TI interface and γ_2 on the sidewall. The FMI layer can be replaced by a magnetic topological insulator.

2.1 Witten Effect

Topological insulators are materials whose d-dimensional bulk is insulating but which host robust, symmetry-protected conducting $d-1$-dimensional surface or edge states arising from a nontrivial topology of their band structure. The addition of an axion term in the electrodynamic Lagrangian models this nontrivial behavior (Qi, Hughes & Zhang, 2008; Rosenberg & Franz, 2010). As a direct result of this additional term, the interface between a TI and a type-II SC can host a topological magneto-electric effect in the form of a fractional charge bound to a vortex, and this is called the Witten effect. The axion term is,

$$S_\theta = \frac{\theta}{8\pi^2}\int d^4x\, F_{\mu\nu}\tilde{F}^{\mu\nu}. \tag{2.1}$$

Here, we loosely follow the work by Nogueira, Nussinov & van den Brink (2016) to find the fractional charge induced by the Witten effect. First, we write the Euler-Lagrange equations for the axion term.

$$\frac{\partial \mathcal{L}_\theta}{\partial A_\lambda} - \partial_\alpha \left(\frac{\partial \mathcal{L}_\theta}{\partial(\partial_\alpha A_\lambda)} \right) = 0 \tag{2.2}$$

The Lagrangian does not depend explicitly on A_λ, reminding ourselves of the form of the field strength $F_{\mu\nu} = \partial_\mu A_\nu - \partial_\nu A_\mu$,

$$\frac{\partial \mathcal{L}_\theta}{\partial A_\lambda} = 0 \tag{2.3}$$

We now compute the derivative of $\mathcal{L}_\theta$ with respect to $\partial_\alpha A_\lambda$, recalling the functional derivative of $F_{\mu\nu}$

$$\frac{\partial F_{\mu\nu}}{\partial(\partial_\alpha A_\lambda)} = \delta^\alpha_\mu \delta^\lambda_\nu - \delta^\alpha_\nu \delta^\lambda_\mu. \tag{2.4}$$

We apply this to compute the variation of the Lagrangian.

$$\begin{aligned} \frac{\partial \mathcal{L}_\theta}{\partial(\partial_\alpha A_\lambda)} &= \frac{\theta e^2}{64\pi^2} \epsilon^{\mu\nu\rho\sigma} \left(\frac{\partial F_{\mu\nu}}{\partial(\partial_\alpha A_\lambda)} F_{\rho\sigma} + F_{\mu\nu} \frac{\partial F_{\rho\sigma}}{\partial(\partial_\alpha A_\lambda)} \right) \\ &= \frac{\theta e^2}{64\pi^2} \epsilon^{\mu\nu\rho\sigma} \left((\delta^\alpha_\mu \delta^\lambda_\nu - \delta^\alpha_\nu \delta^\lambda_\mu) F_{\rho\sigma} + F_{\mu\nu} (\delta^\alpha_\rho \delta^\lambda_\sigma - \delta^\alpha_\sigma \delta^\lambda_\rho) \right) \\ &= \frac{\theta e^2}{32\pi^2} \epsilon^{\alpha\lambda\rho\sigma} F_{\rho\sigma}. \end{aligned} \tag{2.5}$$

Next, we take the derivative of this expression with respect to x^α

$$\begin{aligned} \partial_\alpha \left(\frac{\partial \mathcal{L}_\theta}{\partial(\partial_\alpha A_\lambda)} \right) &= \partial_\alpha \left(\frac{\theta e^2}{32\pi^2} \epsilon^{\alpha\lambda\rho\sigma} F_{\rho\sigma} \right) \\ &= \frac{e^2}{32\pi^2} (\partial_\alpha \theta) \epsilon^{\alpha\lambda\rho\sigma} F_{\rho\sigma} + \frac{\theta e^2}{32\pi^2} \epsilon^{\alpha\lambda\rho\sigma} \partial_\alpha F_{\rho\sigma} \end{aligned} \tag{2.6}$$

Substituting back into the Euler-Lagrange equation gives

$$\frac{-e^2}{32\pi^2}\left((\partial_\alpha\theta)\epsilon^{\alpha\lambda\rho\sigma}F_{\rho\sigma}+\theta\epsilon^{\alpha\lambda\rho\sigma}\partial_\alpha F_{\rho\sigma}\right)=0. \tag{2.7}$$

We want to look at the charge induced by the axion term; therefore, we should find out what the modified Gauss' Law is. To obtain the charge density, we consider terms involving F_{0i} and ∂_0, and rearrange to get the modification to the Gauss' Law in terms of the familiar electric and magnetic fields,

$$\frac{e^2}{8\pi^2}\nabla\theta\cdot\mathbf{B}=J^0_\theta. \tag{2.8}$$

Or the full form, with the original $\nabla\cdot\mathbf{E}=\rho$ added reads

$$\nabla\cdot\mathbf{E}+\frac{e^2}{8\pi^2}\nabla\theta\cdot\mathbf{B}=J^0+J^0_\theta. \tag{2.9}$$

Let's assume there is no free charge $J^0=\rho=0$. The SC and the TI are topologically trivial and non-trivial sectors, respectively and the topological term changes at $z=0$ with $\theta=\pi\Theta(z)$ where the $\Theta(z)$ is the Heaviside step function; the axion term reads $\nabla\theta=\pi\delta(z)\hat{z}$. In a type-II SC, the magnetic field only penetrates through vortices and with a flux quanta of $\Phi_0=\frac{2\pi}{e}$. Therefore, the magnetic field enters only through vortex cores. A vortex at $(0,0)$ would result in $\mathbf{B}=\Phi_0\delta^2(x,y)\hat{z}$. At the boundary, the induced charge will be

$$J^0_\theta=\frac{e^2}{8\pi^2}\pi\delta^3(x,y,z)\frac{2\pi}{e}=\frac{e}{4}\delta^3(x,y,z), \tag{2.10}$$

a fractional charge of $e/4$ localized at the interface between TI and SC, at the vortex core.

Section Summary: In this section, we derived the modified Gauss' law in the presence of an axion term for a topological insulator–superconductor interface and showed that a magnetic vortex piercing the interface induces a localized fractional electric charge $e/4$ at the vortex core.

2.2 Topological Spin Associated Fermi Sea Charge

Exchanging two Majorana zero modes (MZMs) from different fermionic modes, denoted $\hat{\gamma}_1$ and $\hat{\gamma}_2$, implements a Clifford gate on the fusion space of Majorana quasiparticles

$$e^{i\theta}\,(1+\hat{\gamma}_1\hat{\gamma}_2)\,. \tag{2.11}$$

The factor $(1+\hat{\gamma}_1\hat{\gamma}_2)$ encodes the non-Abelian part of the exchange. Remarkably, this term is universal, meaning it is independent of the physical platform in which the MZMs are realized. Since physical observables depend only on the modulus of the wavefunction, global phases are usually unobservable, which makes the Abelian phase $e^{i\theta}$ easy to overlook.

Nevertheless, this Abelian phase is fundamental. It characterizes the internal structure and exchange statistics of quasiparticles through the topological spin s, defined via the phase factor $e^{i2\pi s}$ acquired when a quasiparticle is adiabatically rotated around itself (i.e., under a 2π twist or exchange) (Ariad & Grosfeld, 2017; Nava, Egger, Hassler & Giuliano, 2024; Simon, 2023). For reference, bosons and fermions correspond to integer and half-integer values of s, respectively, while anyons can take arbitrary real values $s \in [0,1)$[2].

In particular, the topological spin of vortex-bound MZMs is directly related to the Aharonov–Casher phase (Aharonov & Casher, 1984), the geometric phase acquired when one vortex adiabatically encircles a bound fractional charge (Ariad & Grosfeld, 2017).

We work with a mean-field Bogoliubov de Gennes (BdG) Hamiltonian to model the topological superconductor. For our purposes, it's useful to write the pairing term in real space on a lattice

$$\mathcal{H}(\phi_0) = \sum_{\mathbf{k}} \psi^\dagger_{\mathbf{k}} H_0(\mathbf{k}) \psi_{\mathbf{k}} + \sum_i \Delta_0 e^{i\varphi_i + i\phi_0} \psi_{i\uparrow}\psi_{i\downarrow} + \text{h.c.}, \tag{2.12}$$

where $H_0(\mathbf{k})$ is the band Hamiltonian of the topological materia, φ_i is the spatially varying superconducting phase at site i. Here the spatial dependency of the phase is $\varphi_i = \arctan(y_i/x_i)$, representing a vortex with the core at $(x,y) = (0,0)$. The real space rotation over an angle $\phi_0 \to \phi_0 + \delta\phi_0$, which winds an anti-vortex bound

[2] See (Simon, 2023) for a pedagogical introduction.

MZM around the center vortex, is equivalent to winding the superconductive phase by a global phase rotation over the same angle, see Fig 2.2. Therefore, to study the

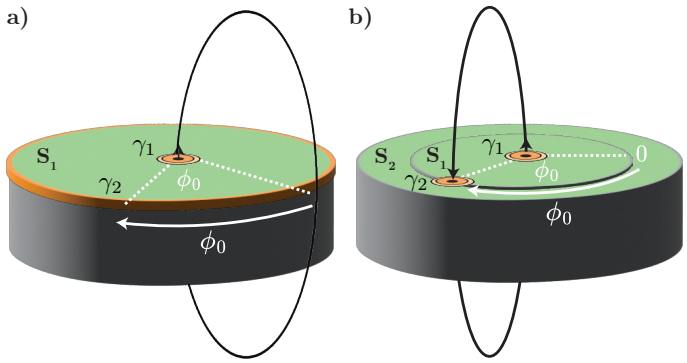

Figure 2.2 Phase winding and vortex circulation equivalence. a) Winding the global superconducting phase in a vortex system is equivalent to b) moving another (anti)vortex around the central vortex.

topological spin of the vortex-bound MZM, we will calculate the geometric phase upon winding the superconductive phase by a global phase rotation. We consider the unitary rotation of the particle-number phase

$$U = \exp\left(i\phi\frac{\hat{N}}{2}\right), \tag{2.13}$$

under which the Hamiltonian transforms as

$$H(\phi) = U\,H(0)\,U^{\dagger}, \tag{2.14}$$

and therefore, the eigenvectors $|\Omega(\phi)\rangle$ of the transformed Hamiltonian are

$$H(\phi)\,U\,|\Omega(0)\rangle = E\,|\Omega(\phi)\rangle\,. \tag{2.15}$$

Thus $|\Omega(\phi)\rangle$ can be obtained by acting with U on the $\phi = 0$ ground state. We write the ground state in BCS form at $\phi = 0$

$$|\mathrm{BCS}_{\phi_0}\rangle = \exp\left(\frac{i\hat{N}\phi_0}{2}\right)|\mathrm{BCS}_0\rangle\,. \tag{2.16}$$

The Berry connection along this adiabatic path is

$$\mathcal{A}(\phi_0) = -i\,\langle \mathrm{BCS}_{\phi_0}|\,\partial_{\phi_0}\,|\mathrm{BCS}_{\phi_0}\rangle\,, \tag{2.17}$$

which gives rise to the geometric phase

$$\int_0^{2\pi}\mathcal{A}(\phi_0)\mathrm{d}\phi_0 = \frac{1}{2}\int_0^{2\pi}\langle\hat{N}\rangle\mathrm{d}\phi_0 = \pi\langle\hat{N}\rangle. \tag{2.18}$$

This leads to the identity

$$\exp(4\pi i s) = \exp(i\pi\langle\hat{N}\rangle). \tag{2.19}$$

Vortex-bound MZMs are known to be Ising anyons, with topological spin $s = 1/16$. We can solve for $\langle\hat{N}\rangle$ with $s = 1/16$, which yields

$$\langle\hat{N}\rangle \equiv \frac{1}{4} \pmod 2, \tag{2.20}$$

indicating a bound fractional charge of $e/4$ in the Fermi sea. When we combine the $-e/4$ charge from the Witten effect with the $e/4$ charge related to the MZM's topological spin, the total net charge becomes zero. The robustness of this charge to local perturbations, therefore its topological protection is discussed in Appendix A.

Section Summary: In this Section, we showed that the topological spin of an MZM is associated with a fractional charge of the Fermi sea. This is an additional charge to the $-e/4$ Witten effect charge discussed in the previous Section, and for the MZMs that we are interested in, has the value of $e/4 \pmod 2$.

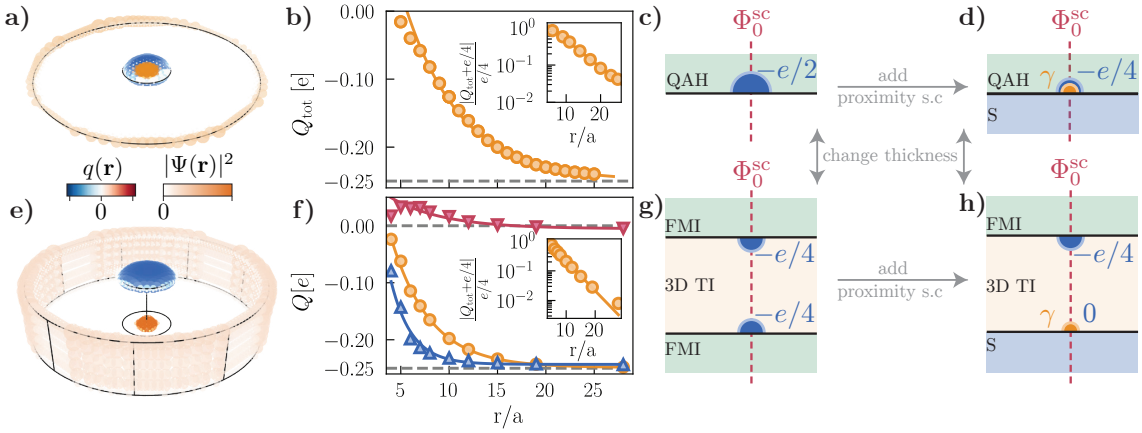

Figure 2.3 Fractional charges and MZM densities in a 2D QAH (top row) and 3D TI (bottom row). a) Charge and MZM densities (one MZM at the center and one at the edge) as a result of a $\Phi_0^{\rm sc} = h/2e$ vortex at the center of a 2D QAH system. b) Integrated total charge density as a function of system size r in units of the lattice space a, inset: relative deviation of integrated charge from $-e/4$. c) A 2D QAH system in the absence of a superconductive pairing potential d) A 2D QAH system in the presence of a superconductive pairing potential. e) As in a) but for a 3D S/3D TI/FMI heterostructure. f) As in b) but for a 3D S/3D TI/FMI heterostructure. Charge integrated on the bottom surface(red up triangle) and the top surface(blue triangle). g) An FMI/3D TI/FMI heterostructure in the absence of a superconductive pairing potential. h) An S/3D TI/FMI heterostructure in the presence of a dominant superconductive pairing potential on the bottom interface.

2.3 Fractional charges in 2D vs 3D.

We now investigate vortex-bound fractional charges in 2D QAH and 3D TI systems, using a tight-binding code[3]. This allows us to highlight fundamental differences in the topological spin of MZMs in true 2D systems versus those arising on the surfaces of 3D topological materials. We begin with a quantum anomalous Hall (QAH) insulator proximitized by a conventional s-wave superconductor. The single-particle Hamiltonian in terms of the two-dimensional momentum $\boldsymbol{k} = (k_x, k_y)$ is

$$H_0^{\rm QAH}(\boldsymbol{k}) = v_F \sin \boldsymbol{k} \cdot \boldsymbol{\sigma}_{\rm 2D} + m(\boldsymbol{k})\sigma_z + \beta\sigma_z - \mu\sigma_0, \tag{2.21}$$

where $\boldsymbol{\sigma}_{\rm 2D} = (\sigma_x, \sigma_y)$, the mass term is $m(\boldsymbol{k}) = m_0 + m_2(2 - \cos k_x - \cos k_y)$, β represents a magnetic exchange field, and μ is the chemical potential (set to zero here for simplicity). For $\Delta_0 \geq |\beta|$, a vortex carrying flux $\Phi_0^{\rm sc}$ binds a MZM at the vortex core and another at the sample edge (Qi, Hughes & Zhang, 2010) [Fig. 2.3(a)]. We

[3]All simulations were performed using Kwant (Groth, Wimmer, Akhmerov & Waintal, 2014); details are provided in Section 2.4, and Appendix A.

also find a fractional charge of $-e/4$ co-localized with the core MZM [Fig. 2.3(b)], which converges exponentially with the system radius r. For small r, hybridization between the MZMs lifts their degeneracy and suppresses the fractional charge, but this overlap decays exponentially with increasing separation.

Next, we turn to the Fu–Kane model on the surface of a 3D topological insulator. The single-particle Hamiltonian for a proximitized 3D TI, in terms of the three-dimensional momentum $\boldsymbol{k} = (k_x, k_y, k_z)$, is

$$H_0^{\mathrm{3DTI}}(\boldsymbol{k}) = v_F \tau_z \sin \boldsymbol{k} \cdot \boldsymbol{\sigma}_{\mathrm{3D}} + M(\boldsymbol{k}) \tau_x \sigma_0 + \beta(z) \tau_0 \sigma_z - \mu \tau_0 \sigma_0, \tag{2.22}$$

where $\boldsymbol{\sigma}_{\mathrm{3D}} = (\sigma_x, \sigma_y, \sigma_z)$, τ_i are Pauli matrices acting on orbital degrees of freedom, and $M(\boldsymbol{k}) = M_0 + M_2(3 - \cos k_x - \cos k_y - \cos k_z)$. The magnetization $\beta(z)$ varies along the vertical (z) direction.

As in the 2D case, this 3D system hosts a vortex-bound MZM at the bottom interface when $\Delta_0 > |\beta|$ (Fu & Kane, 2008), along with a second MZM delocalized along the side surface. However, unlike in 2D QAH systems, the S/3D TI/FMI heterostructure exhibits no fractional charge near the core MZM [Fig. 2.3(e)]. Instead, a fractional charge of $-e/4$ localizes on the top TI/FMI interface, where the vortex flux exits [Fig. 2.3(f)]. This charge also converges exponentially to its quantized value as the system size increases.

In 3D geometry, the neutral MZM and the $-e/4$ fractional charge are spatially separated on opposite surfaces. By increasing the superconducting pairing strength beyond the magnetic coupling on the bottom surface, a fermion fractionalizes into two non-Abelian Ising anyons. The vortex-bound Ising anyon carries a topological spin and the related charge of $e/4$, which is canceled by an opposite $-e/4$ charge from the Witten effect charge of the vortex. This $-e/4$ Abelian anyon effectively "fuses" with the non-Abelian one, yielding a neutral anyon at the bottom interface and leaving a $-e/4$ Abelian anyon at the top surface (Fig. 2.3.h).

Whereas in 2D we see that the MZM co-localizes with a $-e/4$ charge. Here, a 2D QAH can be thought of as a thin 3D TI, wherein the two $-e/4$ Witten charges combine to live on the same surface as a $-e/2$ charge (Asmar, Sheehy & Vekhter, 2018; Zhang, He, Chang, Song, Wang, Chen, Jia, Fang, Dai, Shan, Shen, Niu, Qi, Zhang, Ma & Xue, 2010). Thus, the $e/4$ contribution associated with the topological spin of the MZM combines with the $-e/2$ surface charge to yield a localized Ising anyon carrying a net charge of $-e/4$.

This contrasting behavior of MZMs in effective 2D (QAH) versus 3D (TI) systems provides an experimental knob to tune their topological spin. By adjusting the TI

thickness, one can access the 2D limit with hybridized surfaces or the 3D limit with separated ones. Braiding MZMs in 2D yields an Abelian phase $e^{-i\pi/4}$ (Fig. 2.3.a–d), while in the 3D Fu–Kane heterostructure (Fig. 2.1), the Abelian contribution vanishes (Fig. 2.3.e–h). This tunability offers control over both exchange statistics and topological spin.

Section Summary: We find that in 2D QAH systems the two fractional charges $-e/2$ coming from the Witten effect and $+e/4$ coming from the topological spin of the MZM localize on the same surface and combine into a net $-e/4$ charge coexisting with a vortex-bound MZM. Whereas, in 3D TI geometries the fractional charges spatially separate: the MZM neutralizes the Witten charge on the bottom interface while a $+e/4$ charge localizes on the top surface. This dimensional crossover, from hybridized to spatially separated, provides a tunable handle on the Abelian phase contribution to MZM braiding and the associated topological spin, enabling control over exchange statistics via system thickness and coupling strengths.

2.4 Numerical Methods

In this Section, we discuss the numerical methods used to generate the plots discussed in this work. After briefly introducing the tight-binding Hamiltonian, we describe the construction of the ground state and its associated observables: The particle number expectation value, and the Berry phase under a twist (Section 2.4.1). We then demonstrate the equivalence between the Fermi sea charge and the Berry phase in the Thouless representation (Section 2.4.2). This equivalence is included here for completeness and as a consistency.

We start with a default tight-binding approach. The momentum operator in the real space basis is a derivative; we discretize this operator on a lattice Λ. This is also called the finite difference method. In one dimension, the finite difference of a state defined at a particular x', and a the distance between lattice points, reads

$$\partial_x |x'\rangle = \frac{1}{2a}(|x'+a\rangle - |x'-a\rangle). \tag{2.23}$$

Since this needs to hold for all x in the lattice Λ, the matrix form of the differential

operator reads

$$\hat{\partial}_x = \sum_{x\in\Lambda} \frac{1}{2a}(|x+a\rangle - |x-a\rangle)\langle x|. \tag{2.24}$$

The corresponding band Hamiltonian term is also lattice regularized. Writing $|x\rangle = \sum_k e^{ikx}|k\rangle$ and substituting in the above definitions, the term reads $\sin ak$, rather than k in the continuum theory. These can be generalized to higher dimensions as well; here, we write the two-dimensional operator

$$\sin a\mathbf{k} \Leftrightarrow \frac{i}{2a}\sum_{x,y}|x,y\rangle\left(\langle x+a,y| + \langle x,y+a| - \langle x-a,y| - \langle x,y-a|\right), \tag{2.25}$$

where a is the inter-atomic distance and t is the "hopping" strength. We include the second-order momentum operator for completeness

$$\sum_{i=x,y}(1-\cos ak_i) \Leftrightarrow \frac{-1}{4a^2}\sum_{x,y}|x,y\rangle\left(\langle x+a,y| + \langle x,y+a| + \langle x-a,y| + \langle x,y-a| - 4\langle x,y|\right). \tag{2.26}$$

The pair potential doesn't have a momentum dependence $\Delta_{\mathbf{k}} = \Delta_0$, so the inverse Fourier transform of this would read $\Delta_0\delta(x')$, and this can have a local phase, so in the tight-binding approach, this reads

$$\Delta_{\mathbf{k}} \Leftrightarrow \sum_{x,y}\Delta_0 e^{i\phi(x,y)}|x,y\rangle\langle x,y|. \tag{2.27}$$

Other terms, those without $\mathbf{k}$ dependence, also carry over to the tight-binding Hamiltonian in a similar manner, they can act on other degrees of freedom such as spin and orbital degrees of freedom in which case the matrix entry enters via Kronecker product with the position matrix. Discretized on a lattice of side lengths l_x, l_y, for example, a continuum Hamiltonian of size $(n\times n)$ would have size $(nl_xl_y \times nl_xl_y)$.

We discretize the 2D QAH Hamiltonian (2.21) to obtain the

$$\begin{aligned} H^{\text{QAH}} = &\sum_{\boldsymbol{r}}\begin{pmatrix} (\beta+m_0+2m_2)\sigma_z+\mu & \Delta_0 e^{i\phi(\mathbf{r})} \\ \Delta_0 e^{-i\phi(\mathbf{r})} & (\beta+m_0+2m_2)\sigma_z-\mu \end{pmatrix}|\mathbf{r}\rangle\langle\mathbf{r}| + \\ &\sum_{\boldsymbol{\delta},\mathbf{r}}\begin{pmatrix} \exp i\int_{\mathbf{r}}^{\mathbf{r}+\boldsymbol{\delta}}\boldsymbol{A}\cdot\boldsymbol{dl} & 0 \\ 0 & \exp -i\int_{\mathbf{r}}^{\mathbf{r}+\boldsymbol{\delta}}\boldsymbol{A}\cdot\boldsymbol{dl} \end{pmatrix}\left(t\boldsymbol{\delta}\cdot\boldsymbol{\sigma}+\frac{m_2}{2}\sigma_z\right)|\mathbf{r}+\boldsymbol{\delta}\rangle\langle\mathbf{r}| + h.c. \end{aligned} \tag{2.28}$$

.

We discretize the 3D(M)TI Hamiltonian (2.22) to obtain

$$H^{\mathrm{3DTI}} = \sum_{\boldsymbol{r}} \begin{pmatrix} \beta(\boldsymbol{r})\sigma_z + (m_0+2m_2)\tau_x + \mu & \Delta_0(\boldsymbol{r})e^{i\phi(\boldsymbol{r})} \\ \Delta_0(\boldsymbol{r})e^{-i\phi(\boldsymbol{r})} & \beta(\boldsymbol{r})\sigma_z + (m_0+2m_2)\tau_x - \mu \end{pmatrix} |\boldsymbol{r}\rangle \langle \boldsymbol{r}| +$$

$$\sum_{\boldsymbol{\delta},\boldsymbol{r}} \begin{pmatrix} \exp i\int_{\boldsymbol{r}}^{\boldsymbol{r}+\boldsymbol{\delta}} \boldsymbol{A}\cdot\boldsymbol{dl} & 0 \\ 0 & \exp -i\int_{\boldsymbol{r}}^{\boldsymbol{r}+\boldsymbol{\delta}} \boldsymbol{A}\cdot\boldsymbol{dl} \end{pmatrix} (t\boldsymbol{\delta}\cdot\boldsymbol{\sigma} + m_2\tau_x) |\boldsymbol{r}+\boldsymbol{\delta}\rangle \langle \boldsymbol{r}| . \tag{2.29}$$

The vector potential, which enters the Hamiltonian through minimal coupling $H_0(\mathbf{k}) \to H_0(\mathbf{k} - e\mathbf{A})$, becomes a Peierls phase in the tight-binding approximation. The vector potential describes a magnetic field $\boldsymbol{B} = \Theta(R-\boldsymbol{\rho})\hat{\mathbf{z}}$ where $\boldsymbol{\rho} = x\boldsymbol{x} + y\boldsymbol{y}$ is the radial distance from the vortex core in the center-most plaquette, and R marks the radius of the circular region where the magnetic field acts. Neither depends on the z coordinate. The vector potential reads,

$$\boldsymbol{A} = \begin{cases} \Phi\frac{r}{2\pi R^2}\hat{\boldsymbol{\phi}}, & r < R \\ \Phi\frac{1}{2\pi r}\hat{\boldsymbol{\phi}}, & r > R. \end{cases} \tag{2.30}$$

Where $\Phi = n\Phi_0$ is the total flux is an integer multiple of the superconducting flux quanta, and $\hat{\boldsymbol{\phi}} = -y\hat{\boldsymbol{x}} + x\hat{\boldsymbol{y}}$ is the azimuthal angle around the vortex core at $\mathbf{r}_0 = (0,0)$.

2.4.1 Constructing the ground state and its observables

The tight-binding BdG Hamiltonian $\hat{H}^{\text{t-b}}_{\text{BdG}} = \Psi^\dagger \mathcal{H} \Psi$, with $\mathcal{H}$ giving the Bogoliubov equation reads

$$\hat{H}^{\text{t-b}}_{\text{BdG}} = \begin{pmatrix} \hat{\psi}^\dagger & \hat{\psi} \end{pmatrix} \begin{pmatrix} H_0 & \Delta_0 e^{i\phi} \\ \Delta_0 e^{-i\phi} & -\sigma_y H_0^* \sigma_y \end{pmatrix} \begin{pmatrix} \hat{\psi} \\ \hat{\psi}^\dagger \end{pmatrix}, \tag{2.31}$$

with Fermionic operators in lattice real-space basis $\hat{\psi} = \left(\hat{\psi}_1, \ldots, \hat{\psi}_N\right)^T$, where each index corresponds to a position on the lattice $\mathbf{r}_i \in \Lambda$, and since the single particle Hamiltonian H_0 includes hoppings in-between neighbouring sites, and onsite potentials we can write

$$\hat{H}^{\text{t-b}}_{\text{BdG}} = \sum_{\langle ij \rangle} \hat{\psi}_i^\dagger H_{0,ij} \psi_j + \sum_i \Delta_0 e^{i\phi_i} \psi_i^\dagger \psi_i^\dagger + \text{h.c.}, \tag{2.32}$$

with $\langle ij \rangle$ corresponding to indices pointing to positions in the lattice with either $|\mathbf{r}_i - \mathbf{r}_j| = a$ or $\mathbf{r}_i = \mathbf{r}_j$. We define the Bogoliubov quasi-particle operators as

$$\begin{pmatrix} \hat{\gamma} \\ \hat{\gamma}^\dagger \end{pmatrix} = \begin{pmatrix} U & \bar{V} \\ V & \bar{U} \end{pmatrix} \begin{pmatrix} \hat{\psi} \\ \hat{\psi}^\dagger \end{pmatrix} \tag{2.33}$$

Where $(U, V)^T$ are the positive eigenstates to the Bogoliubov equation,

$$\begin{pmatrix} U^\dagger & V^\dagger \\ \bar{V}^\dagger & \bar{U}^\dagger \end{pmatrix} \begin{pmatrix} H_0 & \Delta_0 e^{i\phi} \\ \Delta_0 e^{-i\phi} & -\sigma_y H_0^* \sigma_y \end{pmatrix} \begin{pmatrix} U & \bar{V} \\ V & \bar{U} \end{pmatrix} = \begin{pmatrix} E & 0 \\ 0 & -E \end{pmatrix}. \tag{2.34}$$

From the electron-hole symmetry (Charge conjugation symmetry) $\mathcal{C} = \sigma_y \nu_y \mathcal{K}$ symmetry we know that $\bar{U} = i\sigma_y U^*$ and $\bar{V} = -i\sigma V^*$. The Thouless representation gives the ground state wave function of the BCS state in an arbitrary basis

$$|\Omega\rangle = A \exp\left(\frac{1}{2}\psi^\dagger Z \psi^{\dagger T}\right)|0\rangle\,. \tag{2.35}$$

We relate the matrices U and V to Z from the condition that the new annihilation operator in the diagonalized basis kills the ground state, i.e. $\gamma_\alpha|\Omega\rangle = 0$.

$$\begin{aligned} \gamma_\alpha|\Omega\rangle &= \left(\sum_i U_{i\alpha}\psi_i + \bar{V}_{i\alpha}\psi_i^\dagger\right)|\Omega\rangle \\ &= \left(\sum_i U_{i\alpha}\psi_i + \bar{V}_{i\alpha}\psi_i^\dagger\right) A e^{\frac{1}{2}\psi^\dagger Z \psi^{\dagger T}}|0\rangle. \end{aligned} \tag{2.36}$$

Using the identity

$$\psi_k e^{\frac{1}{2}\psi^\dagger Z \psi^{\dagger T}}|0\rangle = \sum_j Z_{kj}\psi_j^\dagger e^{\frac{1}{2}\psi^\dagger Z \psi^{\dagger T}}|0\rangle, \tag{2.37}$$

we find

$$\begin{aligned} \gamma_\alpha|\Omega\rangle = \\ \sum_i U_{i\alpha}\psi_i|\Omega\rangle + \sum_i \bar{V}_{i\alpha}\psi_i^\dagger|\Omega\rangle = \\ \sum_{i,j} U_{i\alpha}Z_{ij}\psi_j^\dagger|\Omega\rangle + \sum_i \bar{V}_{i\alpha}\psi_i^\dagger|\Omega\rangle = \\ \sum_j \left(\sum_i U_{i\alpha}Z_{ij} + \bar{V}_{j\alpha}\right)\psi_j^\dagger|\Omega\rangle = \\ \sum_j \left(\sum_i U_{\alpha i}^T Z_{ij} + \bar{V}_{\alpha j}^T\right)\psi_j^\dagger|\Omega\rangle = 0. \end{aligned} \tag{2.38}$$

This expression should vanish for all α, so we get the matrix equation

$$\begin{aligned} U^T Z + \bar{V}^T &= 0 \\ Z &= -(U^{-1})^T \bar{V}^T \\ Z &= \bar{V} U^{-1}. \end{aligned} \tag{2.39}$$

We used the asymmetry of the $Z = -Z^T$ matrix in the last line. We need to normalize the wave function before moving on. We know that Z is an asymmetric matrix; therefore, it can be block diagonalized using a unitary transformation P with

$$Z = P^\dagger D P; \quad D = \begin{pmatrix} 0 & -z_k \\ z_k & 0 \end{pmatrix}, \tag{2.40}$$

where z_k are the eigenvalues of the matrix Z. Expressing the BCS ground state with fermionic operators in this transformed basis, we get

$$|\Omega\rangle = A \exp\left(\frac{1}{2} \sum_k \begin{pmatrix} \eta^\dagger_{2k} & \eta^\dagger_{2k+1} \end{pmatrix} \begin{pmatrix} 0 & -z_k \\ z_k & 0 \end{pmatrix} \begin{pmatrix} \eta^\dagger_{2k} \\ \eta^\dagger_{2k+1} \end{pmatrix} \right) |0\rangle \quad ; \quad \eta^\dagger = P \psi^\dagger. \tag{2.41}$$

Expanding the exponential and keeping in mind that squared fermion operators vanish, we get

$$|\Omega\rangle = A \prod_k \left(1 + z_k \eta^\dagger_{2k} \eta^\dagger_{2k+1} \right) |0\rangle . \tag{2.42}$$

Using the well-known identity for Fermionic Gaussian states, the normalization of this wavefunction is given by

$$\langle \Omega | \Omega \rangle = |A|^2 \prod_k (1 + |z_k|^2)^{1/2} = |A|^2 \det(1 + Z^\dagger Z)^{1/2}. \tag{2.43}$$

The equivalence between the determinant expression and the product expression comes from the fact that z_k are eigenvalues of the matrix Z. Thus, a normalized version of the state is

$$|\Omega\rangle = \frac{1}{\det(1 + Z^\dagger Z)^{1/4}} \exp\left(\sum_{i<j} Z_{ij} \psi^\dagger_i \psi^\dagger_j \right) |0\rangle. \tag{2.44}$$

Using the normalization $U^\dagger U + V^\dagger V = 1$, we get the identity

$$\begin{aligned} Z^\dagger Z &= U^{-1\dagger}\bar{V}^\dagger \bar{V} U^{-1} \\ Z^\dagger Z &= U^{-1\dagger}(1-\bar{U}^\dagger \bar{U})U^{-1} \\ Z^\dagger Z &= U^{-1\dagger}U^{-1} - 1 \\ (Z^\dagger Z + 1)^{-1} &= U^\dagger U = \bar{U}^\dagger \bar{U}. \end{aligned} \tag{2.45}$$

We find that the expectation value of the number operator $\hat{N} = \mathrm{Tr}\, \bar{V}^\dagger \bar{V}$, recalling that $\bar{V}^\dagger \bar{V} = U^\dagger Z^\dagger Z U$, becomes

$$\begin{aligned} \langle \hat{N} \rangle &= \mathrm{Tr}\left[U^\dagger Z^\dagger Z U\right] = \\ &\mathrm{Tr}\left[Z^\dagger Z\, U^\dagger U\right] = \\ &\mathrm{Tr}\left[Z^\dagger Z\,(1+Z^\dagger Z)^{-1}\right]. \end{aligned} \tag{2.46}$$

2.4.2 Fermi sea charge equivalence in Thouless representation

Using Thouless representation allows us to work out the phase winding algebra explicitly. The Heuristic is this: Because $\exp i\phi_0 \hat{N}/2$ is a global phase rotation, the many-body state must describe the same state regardless of ϕ_0.

$$\begin{aligned} &\exp\left(i\phi_0/2 \sum_k \psi_k^\dagger \psi_k\right) \exp\left(\sum_{i<j} Z_{ij}(0)\psi_i^\dagger \psi_j^\dagger\right)|0\rangle \\ &= \exp\left(\sum_{i<j} Z_{ij}(\phi_0)\psi_i^\dagger\, e^{-i\phi_0/2}\psi_j^\dagger\, e^{-i\phi_0/2}\right)|0\rangle \end{aligned} \tag{2.47}$$

The second line is easily seen via considering that $\Delta_0 \to \Delta_0 e^{i\phi_0}$ is equivalently $\psi \to e^{i\phi_0/2}\psi$ since $\Delta = \langle \psi\, \psi \rangle$. But concretely we can show this by expanding the exponential and working out the algebra for unitary transformations $U \exp A = \exp UAU^\dagger$ on the ground state,

$$|\Omega(0)\rangle = \exp\left(\sum_{i<j} Z_{ij}\, \psi_i^\dagger \psi_j^\dagger\right)|0\rangle\,. \tag{2.48}$$

Applying U gives the ϕ-dependent ground state

$$|\Omega(\phi)\rangle = U \exp\left(\sum_{i<j} Z_{ij}\, \psi_i^\dagger \psi_j^\dagger\right)|0\rangle\,. \tag{2.49}$$

Since the vacuum satisfies $U|0\rangle = e^{i\phi\hat{N}/2}|0\rangle = |0\rangle$, we can insert an identity $U^\dagger U$ in between the ket and the Cooper pair creation operators to get

$$|\Omega(\phi)\rangle = U \exp\left(\sum_{i<j} Z_{ij}\,\psi_i^\dagger \psi_j^\dagger\right) U^\dagger |0\rangle\,. \tag{2.50}$$

Then, we expand the exponential in a power series and conjugate each creation operator by U, recalling $[\psi_k^\dagger, \hat{N}] = \psi_k^\dagger$ and using Baker-Campbell-Hausdorff formula, we get

$$U\,(\psi_i^\dagger \psi_j^\dagger)\,U^\dagger = e^{i\phi}\,\psi_i^\dagger \psi_j^\dagger. \tag{2.51}$$

Every pairing therefore, acquires the same phase factor $e^{i\phi}$, so the entire pairing matrix transforms as

$$Z(\phi) = e^{i\phi}\,Z(0). \tag{2.52}$$

Differentiating $Z(\phi)$ with respect to ϕ gives

$$\frac{\partial Z(\phi)}{\partial \phi} = i\,Z(\phi). \tag{2.53}$$

Using the definition of the Berry connection, called the Read's formula (Read, 2009)

$$\mathcal{A} = \frac{-i}{2}\,\mathrm{Tr}\left[\,Z^\dagger Z'(1+Z^\dagger Z)^{-1}\right], \tag{2.54}$$

and substituting $Z' = iZ$ yields

$$\mathcal{A} = \frac{1}{2}\,\mathrm{Tr}\left[\,Z^\dagger Z(1+Z^\dagger Z)^{-1}\right]. \tag{2.55}$$

Finally, recognizing the expression for the expectation value of the number operator, $\mathrm{Tr}[\,Z^\dagger Z(1+Z^\dagger Z)^{-1}] = \langle\hat{N}\rangle$, we obtain

$$\mathcal{A} = \frac{1}{2}\,\langle\hat{N}\rangle. \tag{2.56}$$

This establishes the equivalence between the topological spin and the Fermi-sea charge. Nevertheless, we can compute the derivative using the finite difference method, and find that the difference between the Berry connection and the Fermi sea charge, i.e., the absolute error, is of the order 10^{-5} as can be seen in Fig 2.4.

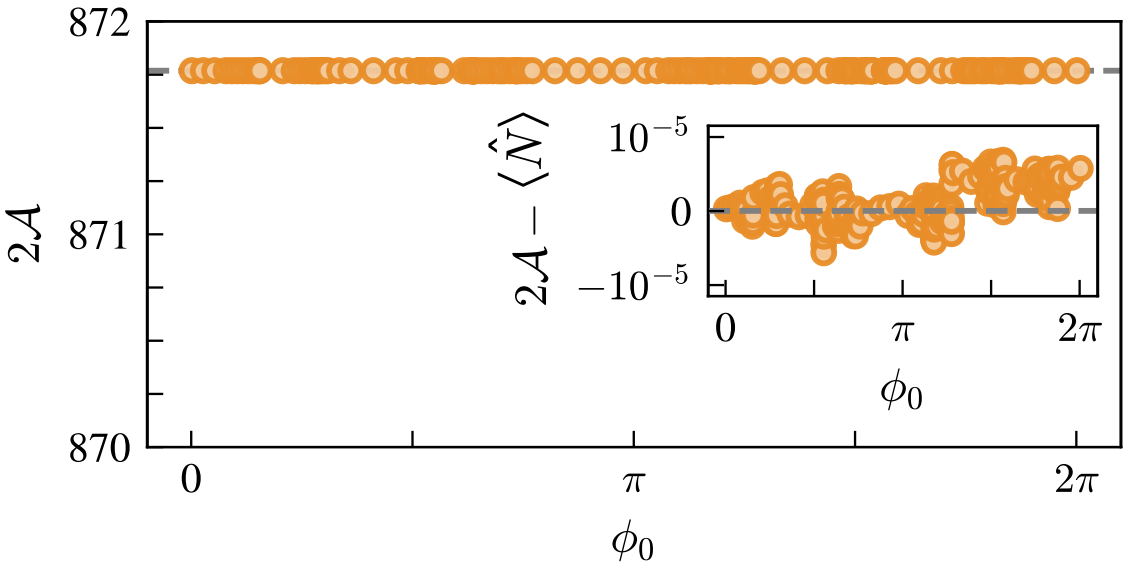

Figure 2.4 Fractional charges and Berry connection. Twice the Berry connection $2\mathcal{A}$ (orange circles) and the number operator expectation value $\langle \hat{N} \rangle$ (dashed gray line) as a function of superconducting phase ϕ_0, for an S/3D TI/FMI heterostructure with an exponentially increasing (decreasing) magnetization (pair potential) from the bottom interface. Inset: deviation of $2\mathcal{A}$ from $\langle \hat{N} \rangle$.

3. OBSERVABLE SIGNATURES OF TOPOLOGICAL SPIN

In this Chapter, we propose a concrete setup to probe the fractional topological spin via vortex interference, and to demonstrate that the quarter fractional charge has observational signatures. After introducing the setup, we derive the Cirquit-QED [1] Hamiltonian and discuss the observable signature of topological spin of MZMs in Section 3.1. Next, we discuss how to calculate the quantities above in Section 3.2.

We propose a generic vortex interference experiment setup. In these experiments (Bell, Zhang, Ioffe & Gershenson, 2016; de Graaf, Skacel, Hönigl-Decrinis, Shaikhaidarov, Rotzinger, Linzen, Ziegler, Hübner, Meyer, Antonov, Il'ichev, Ustinov, Tzalenchuk & Astafiev, 2018; Elion, Wachters, Sohn & Mooij, 1993; Hassler, Akhmerov, Hou & Beenakker, 2010; Randeria, Hazard, Di Paolo, Azar, Hays, Ding, An, Gingras, Niedzielski, Stickler, Grover, Yoder, Schwartz, Oliver & Serniak, 2024; Reznik & Aharonov, 1989; Van Wees, 1990), moving vortices interfere around a charged island, and their interference is modulated due to the Aharonov-Casher effect (Aharonov & Casher, 1984). In our case, Josephson vortices circle a superconducting island charged by the S/3D TI/FMI heterostructure (Fig. 2.1), embedded between two superconducting leads S_1, S_2 (phases ϕ_1, ϕ_2), as shown in Fig. 3.1.a. Each vortex threading the structure induces a fractional charge $e/4$ on the bottom S/3D TI interface, giving $q_\Phi = \frac{e}{4}\Phi/\Phi_0$. The top $-e/4$ charge, spatially separated, remains electrically isolated by design.

3.1 Deriving the circuit QED Hamiltonian

We model the island as a Cooper pair box, with charge $2e\hat{n}$ and conjugate phase $\hat{\theta}$, satisfying $[\hat{\theta}, \hat{n}] = i$. Replacing the global phase $\phi_0 \to \hat{\theta}$ in the BdG Hamiltonian

[1] For a pedagogical introduction to the subject see the lecture notes (Girvin, Devoret & Schoelkopf, 2009), particularly Section 3. and 4.

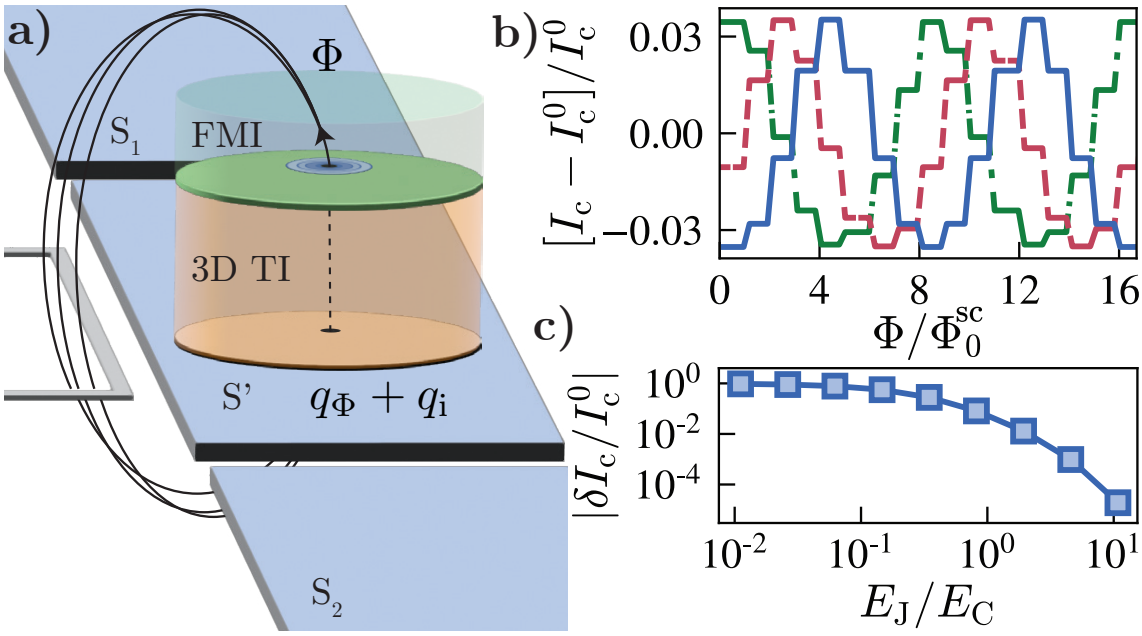

Figure 3.1 Fractional charge experimental signature. a) A double Josephson junction set-up of two superconductors S_1 and S_2 with phases $\varphi_{1,2}$ coupled via a superconducting charge island S' with phase $\theta = (\varphi_1 - \varphi_2)/2$. The island consists of the S/3D TI/FMI heterostructure c.q. Fig. 2.1. The island gets charged through a flux gate (q_Φ) and it can additionally have an image charge (q_i). b) Mean subtracted critical current response as a function of the number of admitted vortices on the island for $q_\mathrm{i} = 0$ (solid blue line), 0.5e (dashed red line), and 1e (dash-dot green line). The ratio of the Josephson energy, E_J, over the capacitive energy, E_C was 1.25. c) Strength of oscillating critical current signal Eq. (3.11), relative to its mean as a function of the $E_\mathrm{J}/E_\mathrm{C}$.

leads to

$$\mathcal{H}_F = \sum_{\mathbf{k}} \psi^\dagger_{\mathbf{k}} H_0(\mathbf{k}) \psi_{\mathbf{k}} + \sum_i \Delta_0 e^{i\varphi_i + i\hat{\theta}} \psi_{i\uparrow}\psi_{i\downarrow} + h.c.. \tag{3.1}$$

Here, $e^{i\hat{\theta}}\psi_{i\uparrow}\psi_{i\downarrow}$ adds a Cooper pair to the island with the coherent phase charging operator $e^{i\hat{\theta}}$, while removing two electrons from the topological material. The top part of the 3D TI is electrically isolated, therefore the total island charge is $q = q_\Phi + q_\mathrm{i}$, where q_Φ is set by the number of vortices, and q_i is an image charge.

In addition to the island we consider two other superconducting subsystems, superconducting leads (1) and (2), as seen in Fig 3.1.a. Each subsystem is described by a phase operator and its conjugate Cooper-pair number operator. The canonical commutator relations are

$$[\hat{\varphi}_i, \hat{N}_j] = i\,\delta_{ij}, \qquad [\hat{\theta}, \hat{n}] = i, \tag{3.2}$$

with $i, j \in \{1,2\}$ and where $(\hat{\theta}, \hat{n})$ denote the island phase and Cooper-pair number.

Operators of different subsystems commute, e.g. $[\hat{\varphi}_i, \hat{n}] = 0$. The Josephson coupling between the island and lead i has the operator form

$$\hat{H}_{J,i} = -\frac{E_{J,i}}{2}\Big(e^{i(\hat{\varphi}_i - \hat{\theta})} + e^{-i(\hat{\varphi}_i - \hat{\theta})}\Big) = -E_{J,i}\cos\Big(\hat{\varphi}_i - \hat{\theta}\Big), \tag{3.3}$$

where $e^{i\hat{\varphi}_i}$ and $e^{\pm i\hat{\theta}}$ are the charge-raising/lowering operators on the corresponding subsystem, and correspond to Cooper pair tunneling to and fro the island to the i'th lead contributing an energy $E_{J,i}$ to the dynamics. For identical junctions ($E_{J,1} = E_{J,2} \equiv E_J$) the total Josephson Hamiltonian reads

$$\hat{H}_J = -E_J\Big[\cos(\hat{\varphi}_1 - \hat{\theta}) + \cos(\hat{\varphi}_2 - \hat{\theta})\Big]. \tag{3.4}$$

Using the trigonometric identity $\cos a + \cos b = 2\cos\left(\frac{a+b}{2}\right)\cos\left(\frac{a-b}{2}\right)$ with $a = \hat{\varphi}_1 - \hat{\theta}$ and $b = \hat{\varphi}_2 - \hat{\theta}$ one obtains

$$\hat{H}_J = -2E_J\cos\Big(\frac{\hat{\varphi}_1 + \hat{\varphi}_2}{2} - \hat{\theta}\Big)\cos\Big(\frac{\hat{\varphi}_1 - \hat{\varphi}_2}{2}\Big). \tag{3.5}$$

We express the Hamiltonian in terms of the phase-difference operators $\hat{\phi}_1$ and $\hat{\phi}_2$ introduced in the paper. These are defined in relation to the phase operators as

$$\hat{\phi}_1 = \hat{\theta} - \hat{\varphi}_1, \qquad \hat{\phi}_2 = \hat{\varphi}_2 - \hat{\theta}. \tag{3.6}$$

With this, the Hamiltonian takes the form

$$\hat{H}_J = -2E_J\cos\Big(\frac{\hat{\phi}_1 - \hat{\phi}_2}{2}\Big)\cos\Big(\frac{\hat{\phi}_1 + \hat{\phi}_2}{2}\Big). \tag{3.7}$$

The island charging energy is given by the capacitive coupling

$$\hat{H}_C = \frac{(2e\hat{n} - q)^2}{2C}, \tag{3.8}$$

where q denotes the total offset charge (gate-induced plus any topological image charge) and C the capacitive coupling constant. The effective Hamiltonian is

$$\hat{H} = \frac{(2e\hat{n} - q)^2}{2C} - 2E_J\cos\Big(\frac{\hat{\phi}_1 - \hat{\phi}_2}{2}\Big)\cos\Big(\frac{\hat{\phi}_1 + \hat{\phi}_2}{2}\Big) \tag{3.9}$$

In the experimentally relevant limit of large superconducting reservoirs, the lead phases may be treated as classical parameters, and the operator $\hat{\phi}_1 + \hat{\phi}_2$ can be replaced by the classical variable φ_T. We can relabel $\frac{\hat{\phi}_1 - \hat{\phi}_2}{2} \to \theta$. It can be easily shown that $[\frac{\hat{\phi}_1 - \hat{\phi}_2}{2}, \hat{n}] = i$, and this relabeling is a mere phase shift. As a result, the

Cooper pair box Hamiltonian becomes

$$H = \frac{(2e\hat{n} - q)^2}{2C} - 2E_J \cos(\varphi_T/2)\cos\theta. \tag{3.10}$$

The critical current oscillates as a function of q, enabling detection of fractional charges and associated topological spin via interference, as in Ref. (Friedman & Averin, 2002). We compute the critical current in the single-arm setup as $I_{\rm sc}(\varphi_{\rm T}) = \frac{dE_0}{d\varphi_{\rm T}}$, where $E_0(\varphi_{\rm T})$ is the ground state energy of Eq. (3.10). As shown in Fig. 3.1.b, $I_{\rm sc}$ exhibits quantized plateaus that depend on the number of admitted vortices $n_\Phi = \Phi/\Phi_0^{\rm sc} \in \mathbb{N}$, and is periodic with $n_\Phi \mod 8$.

$$I^{\rm c} = I_0^{\rm c} + \delta I^{\rm c} \cos\left(\frac{\pi q_\Phi + q_{\rm i}}{e}\right), \tag{3.11}$$

with $q_\Phi = \frac{e n_\Phi}{4}$ the vortex-induced fractional charge and $q_{\rm i}$ a tunable image charge. The modulation amplitude $\delta I^{\rm c}$ is maximized in the weak coupling regime $E_C \gg E_J$ (Bozkurt & Fatemi, 2023) (Fig. 3.1.c).

Most importantly, the eight quantized current plateaus $I_i^{\rm c}$ obey four universal relations

$$\begin{aligned} I_{\rm i}^{\rm c} &= (I_{\rm i+1}^{\rm c} - I_{\rm i+3}^{\rm c})/\sqrt{2}, \qquad \text{for i} = 0{,}4, \\ I_{\rm i}^{\rm c} &= (I_{\rm i-1}^{\rm c} + I_{\rm i+1}^{\rm c})/\sqrt{2}, \qquad \text{for i} = 2{,}6, \end{aligned} \tag{3.12}$$

These quantized plateau values provide a robust experimental signature; they are insensitive to random vortex entry and phase slips, both of which can obscure the $\delta I^{\rm c}$ oscillations but not the quantized values of $I^{\rm c}$.

Section Summary: In this Section, we propose a vortex interference experiment to detect signatures of topological spin of MZMs. We derive the circuit-QED Hamiltonian of the experiment setup, and find that the critical current curves exhibit plateaus quantized by the number of flux quanta admitted in the TI-SC setup. Furthermore, we identify that these plateaus are related to each other in a way that is unaffected by experimental noise.

3.2 Circuit QED Hamiltonian as a Tight-Binding Model

To study the quantum dynamics of the superconducting island, we model the Cooper pair box using a circuit QED Hamiltonian given by Eq. (3.10), which we reproduce here for clarity

$$H = \frac{(2e\hat{n} - q)^2}{2C} - 2E_J \cos\left(\frac{\varphi_T}{2}\right)\cos\theta. \tag{3.13}$$

Here, n is the number of Cooper pairs on the island, $\theta = (\phi_1 - \phi_2)/2$ is the conjugate phase variable, and $[\theta, n] = i$. To solve this Hamiltonian numerically, we treat it as a tight-binding model in the θ basis. We discretize θ, which is a compact variable defined on the interval $[-\pi, \pi)$,

$$|\theta\rangle = |\frac{\pi}{N}k\rangle \equiv |k\rangle\,, \tag{3.14}$$

with $k \in \mathbb{Z}$ defined in the interval $[-N, N-1]$. In this basis, the number operator $\hat{n}$ acts as a hopping term, while the $\cos\theta$ term acts as an onsite potential

$$\hat{n}^2 |k\rangle = \frac{1}{4}\left(|k+1\rangle + |k-1\rangle - 2|k\rangle\right), \tag{3.15}$$

$$\cos\hat{\theta}\,|k\rangle = \cos(\frac{\pi}{N}k)\,|k\rangle\,. \tag{3.16}$$

The induced charge q enters as a Peierls phase on the discrete differential operator, and we rewrite the Hamiltonian as a one-dimensional tight-binding model in the k-basis

$$H(q, \varphi_T) = \sum_k \left[\frac{1}{4C}\left(e^{-i\frac{q}{2C}}|k+1\rangle + e^{i\frac{q}{2C}}|k-1\rangle - 2|k\rangle\right)\langle k| - E_J \cos\left(\frac{\varphi_T}{2}\right)\cos\left(\frac{\pi}{N}k\right)|k\rangle\langle k| + \text{h.c.}\right]. \tag{3.17}$$

This Hamiltonian, which acts on a $2N$ dimensional Hilbert space, is diagonalized numerically with N large enough to ensure convergence. The ground state energy $E_0(\varphi_T)$ obtained from exact diagonalization is then used to compute the critical current via

$$I_{\text{sc}}(\varphi_T) = \frac{dE_0}{d\varphi_T}, \tag{3.18}$$

which is computed via finite difference.

4. SUMMARY AND CONCLUSION

In this thesis, we have demonstrated that the topological spin of Majoranas in SC-TI heterostructures is directly linked to a fractional Fermi-sea charge. We showed that this fractional charge can be either isolated from or fused with a Majorana mode to modify its topological spin. Furthermore, we established that the effects of this fractional Fermi-sea charge, and consequently, the topological spin, can be directly detected through a vortex interference experiment.

We have derived the analytical expressions for the quantities of interest to this work. Furthermore, we provide sufficient methodological details to enable reproduction of the figures presented in this thesis as well as in the associated preprint (de Wit et al., 2025).

For future work, we identify two natural directions. First, an important step is the calculation of the full exchange term (the non abelian part) between a vortex MZM and an anti-vortex MZM. This requires evaluating the time evolution using the Dyson series, a task that is computationally strenuous. Progress along this research direction may motivate the development of more efficient algorithms, which could subsequently be of use to the broader physics community.

Second, we aim to extend the framework beyond the simplified setting considered here. While our analysis focuses on s-wave superconductivity and first-order topological insulators, future work should incorporate real-world complexities such as disorder and finite-temperature effects, as well as more exotic features including higher-order topology, Weyl semimetals, spin–orbit coupling, and unconventional superconducting pairings.

BIBLIOGRAPHY

Aharonov, Y. & Casher, A. (1984). Topological Quantum Effects for Neutral Particles. *Physical Review Letters*, *53*(4), 319–321. Publisher: American Physical Society.

Ariad, D. & Grosfeld, E. (2017). Signatures of the topological spin of Josephson vortices in topological superconductors. *Physical Review B*, *95*(16), 161401. Publisher: American Physical Society.

Asmar, M. M., Sheehy, D. E., & Vekhter, I. (2018). Topological phases of topological-insulator thin films. *Physical Review B*, *97*(7), 075419. Publisher: American Physical Society.

Beenakker, C. (2020). Search for non-Abelian Majorana braiding statistics in superconductors. *SciPost Physics Lecture Notes*, 15.

Beenakker, C. W. J. (2013). Search for Majorana fermions in superconductors. *Annual Review of Condensed Matter Physics*, *4*(1), 113–136. arXiv: 1112.1950.

Bell, M., Zhang, W., Ioffe, L., & Gershenson, M. (2016). Spectroscopic Evidence of the Aharonov-Casher Effect in a Cooper Pair Box. *Physical Review Letters*, *116*(10), 107002. Publisher: American Physical Society.

Bozkurt, A. M. & Fatemi, V. (2023). Josephson tunnel junction arrays and Andreev weak links: linked by a single energy-phase relation. In *Spintronics XVI*, (pp.$\tilde{3}$7). arXiv:2408.06462 [cond-mat].

Caroli, C., De Gennes, P., & Matricon, J. (1964). Bound fermion states on a vortex line in a type ii superconductor. *Physics Letters*, *9*(4), 307–309.

Castagnoli, G. & Rasetti, M. (1993). The notions of symmetry and computational feedback in the paradigm of steady, simultaneous quantum computation. *International Journal of Theoretical Physics*, *32*(12), 2335–2347.

Cook, A. & Franz, M. (2011). Majorana fermions in a topological-insulator nanowire proximity-coupled to an s-wave superconductor. *Physical Review B*, *84*(20), 201105. Publisher: American Physical Society.

de Graaf, S. E., Skacel, S. T., Hönigl-Decrinis, T., Shaikhaidarov, R., Rotzinger, H., Linzen, S., Ziegler, M., Hübner, U., Meyer, H.-G., Antonov, V., Il'ichev, E., Ustinov, A. V., Tzalenchuk, A. Y., & Astafiev, O. V. (2018). Charge quantum interference device. *Nature Physics*, *14*(6), 590–594. Publisher: Nature Publishing Group.

de Wit, S. R., Duman, E., Bozkurt, A. M., Brinkman, A., & Adagideli, I. (2025). Manipulating the topological spin of majoranas.

Elion, W. J., Wachters, J. J., Sohn, L. L., & Mooij, J. E. (1993). Observation of

the Aharonov-Casher effect for vortices in Josephson-junction arrays. *Physical Review Letters*, *71*(14), 2311–2314.

Friedman, J. R. & Averin, D. V. (2002). Aharonov-Casher-Effect Suppression of Macroscopic Tunneling of Magnetic Flux. *Physical Review Letters*, *88*(5), 050403. Publisher: American Physical Society.

Fu, L. & Kane, C. L. (2008). Superconducting Proximity Effect and Majorana Fermions at the Surface of a Topological Insulator. *Physical Review Letters*, *100*(9), 096407. Publisher: American Physical Society.

Girvin, S. M., Devoret, M. H., & Schoelkopf, R. J. (2009). Circuit qed and engineering charge-based superconducting qubits. *Physica Scripta*, *2009*(T137), 014012.

Groth, C. W., Wimmer, M., Akhmerov, A. R., & Waintal, X. (2014). Kwant: a software package for quantum transport. *New Journal of Physics*, *16*(6), 063065.

Hassler, F., Akhmerov, A. R., Hou, C.-Y., & Beenakker, C. W. J. (2010). Anyonic interferometry without anyons: how a flux qubit can read out a topological qubit. *New Journal of Physics*, *12*(12), 125002.

Ivanov, D. A. (2001). Non-Abelian Statistics of Half-Quantum Vortices in p-Wave Superconductors. *Physical Review Letters*, *86*(2), 268–271. Publisher: American Physical Society.

Jackiw, R. & Rossi, P. (1981). Zero modes of the vortex-fermion system. *Nuclear Physics B*, *190*(4), 681–691.

Kitaev, A. Y. (2003). Fault-tolerant quantum computation by anyons. *Annals of Physics*, *303*(1), 2–30. arXiv: quant-ph/9707021.

Lahtinen, V. & Pachos, J. K. (2017). A Short Introduction to Topological Quantum Computation. *SciPost Physics*, *3*(3), 021. arXiv: 1705.04103.

Lutchyn, R. M., Bakkers, E. P. a. M., Kouwenhoven, L. P., Krogstrup, P., Marcus, C. M., & Oreg, Y. (2018). Majorana zero modes in superconductor–semiconductor heterostructures. *Nature Reviews Materials*, *3*(5), 52–68. Publisher: Nature Publishing Group.

Nava, A., Egger, R., Hassler, F., & Giuliano, D. (2024). Non-Abelian Anyon Statistics through ac Conductance of a Majorana Interferometer. *Physical Review Letters*, *133*(14), 146604.

Nayak, C., Simon, S. H., Stern, A., Freedman, M., & Das Sarma, S. (2008). Non-Abelian anyons and topological quantum computation. *Reviews of Modern Physics*, *80*(3), 1083–1159. Publisher: American Physical Society.

Nogueira, F. S., Nussinov, Z., & van den Brink, J. (2016). Josephson currents induced by the witten effect. *Phys. Rev. Lett.*, *117*, 167002.

Qi, X.-L., Hughes, T. L., & Zhang, S.-C. (2008). Topological field theory of time-reversal invariant insulators. *Phys. Rev. B*, *78*, 195424.

Qi, X.-L., Hughes, T. L., & Zhang, S.-C. (2010). Chiral topological superconductor from the quantum Hall state. *Physical Review B*, *82*(18), 184516. Publisher: American Physical Society.

Randeria, M. T., Hazard, T. M., Di Paolo, A., Azar, K., Hays, M., Ding, L., An, J., Gingras, M., Niedzielski, B. M., Stickler, H., Grover, J. A., Yoder, J. L., Schwartz, M. E., Oliver, W. D., & Serniak, K. (2024). Dephasing in Fluxonium Qubits from Coherent Quantum Phase Slips. *PRX Quantum*, *5*(3), 030341.

Read, N. (2009). Non-Abelian adiabatic statistics and Hall viscosity in quantum Hall states and p x + i p y paired superfluids. *Physical Review B*, *79*(4), 045308.

Read, N. & Green, D. (2000). Paired states of fermions in two dimensions with breaking of parity and time-reversal symmetries and the fractional quantum Hall effect. *Physical Review B*, *61*(15), 10267–10297.

Reznik, B. & Aharonov, Y. (1989). Question of the nonlocality of the Aharonov-Casher effect. *Physical Review D*, *40*(12), 4178–4183. Publisher: American Physical Society.

Rosenberg, G. & Franz, M. (2010). Witten effect in a crystalline topological insulator. *Phys. Rev. B*, *82*, 035105.

Simon, S. H. (2023). *Topological Quantum*. Oxford, New York: Oxford University Press.

Van Wees, B. J. (1990). Aharonov-Bohm–type effect for vortices in Josephson-junction arrays. *Physical Review Letters*, *65*(2), 255–258.

Yazdani, A., von Oppen, F., Halperin, B. I., & Yacoby, A. (2023). Hunting for majoranas. *Science*, *380*(6651), eade0850.

Zhang, Y., He, K., Chang, C.-Z., Song, C.-L., Wang, L.-L., Chen, X., Jia, J.-F., Fang, Z., Dai, X., Shan, W.-Y., Shen, S.-Q., Niu, Q., Qi, X.-L., Zhang, S.-C., Ma, X.-C., & Xue, Q.-K. (2010). Crossover of the three-dimensional topological insulator Bi2Se3 to the two-dimensional limit. *Nature Physics*, *6*(8), 584–588. Publisher: Nature Publishing Group.

APPENDIX

Tight-Binding details

Here we provide the simulation parameters used to create the figures included in this thesis. We work with different z dependency for β and Δ_0. The relevant case is when they dominate the other on opposing surfaces. We choose an exponentially decaying form for these functions. These look like $f(z) = ce^{-z/\xi}$ and $f(z) = ce^{-(h-z)/\xi}$ in the case that they dominate in the bottom surface, and at the top surface, respectively. Here ξ is a decay constant and h is the height of the system.

Table A.1 Tight-binding parameters used in each figure. The z_{r} variable indicates that it is in decreasing order from $h-1$ to 0. All parameters in units of the in-plane hopping parameter t.

Figure	Geometry (r,R,h) [a]	Mass	$\beta(z)$	$\Delta(z)$	t_z
2	(6,3,4)	$M_0 = -1.5$, $M_2 = 1.65$	$0.5e^{-z_{\mathrm{r}}/1.5}$	$0.85e^{-z/1.5}$	1/2
3.a,b	(28,4,-) for 3.a & (r,4,-) for 3.b	$M_0 = 0$, $M_2 = -1.35$	0.12	0.61	-
3.e,f	(18,4,6) for 3.e & (r,4,4) for 3.f	$M_0 = -1.5$, $M_2 = 1.65$	$[0,0,0,0.5]$	$[0.7,0,0,0]$	1/2
4.a	(8,3,4)	$M_0 = -1.5$, $M_2 = 1.65$	$[0,0,0,0.5]$	$[0.7,0,0,0]$	1/2
4.b	(16,4,4)	$M_0 = -1.3$, $M_2 = 1.43$	$[0,0,0,0.5]$	$[0.85,0,0,0]$	1/2

Fractional Charge Robustness

We investigate the stability of fractional vortex charges against disorder by adding onsite disorder of strength $\delta\mu$ to the electrochemical potential and computing the induced vortex charge for an ensemble of $N = 1000$ realizations. Figure A.1(a) shows that the induced charges remain stable at $-e/4$ with small fluctuations (one standard deviation) even for strong disorder $\delta\mu \lesssim t$, where t is the characteristic energy scale.

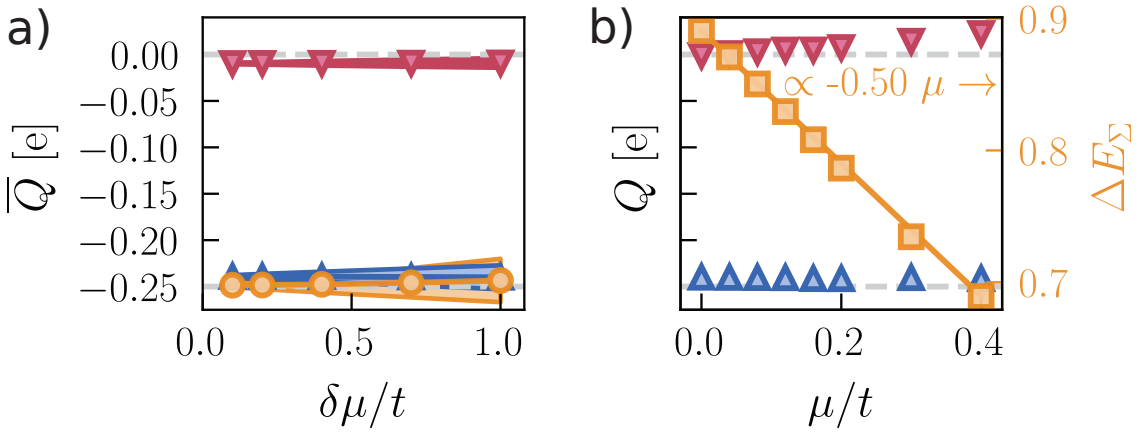

Figure A.1 Fractional charge robustness in a FMI/3D TI/S heterostructure. a) The ensemble ($N = 1000$) averaged accumulated bottom (red down triangle), top (blue up triangle), and total (orange circle) charge as a function of chemical potential disorder strength $\delta\mu/t$, normalized by the hopping strength. Shaded colors correspond to one standard deviation from the mean. b) As a function of the chemical potential μ/t, normalized by the hopping strength, the left y-axis (ticks shared with panel a).) shows the bottom and top charges. The right y-axis (orange squares) shows the background subtracted total occupied energy.

Figure A.1.b demonstrates robustness against variations in the average chemical potential μ, with fractional charges maintaining their values of approximately 0 and $-e/4$ for bottom and top charges respectively. The chemical potential dependence also enables an alternative charge calculation via the Hellmann-Feynman theorem:

$$\frac{\mathrm{d}\Delta E_\Sigma}{\mathrm{d}\mu} = \left\langle \frac{\mathrm{d}\mathcal{H}}{\mathrm{d}\mu} \right\rangle_{\mathrm{vrtx}} - \left\langle \frac{\mathrm{d}\mathcal{H}}{\mathrm{d}\mu} \right\rangle_{\mathrm{bkg}}, \tag{A.1}$$

where ΔE_Σ is the difference in total occupied energy between vortex and background states. Since $\langle \hat{N} \rangle = \langle (\nu_0 + \nu_z)/2 \rangle$ and $\langle \nu_0 \rangle_{\mathrm{vrtx}} - \langle \nu_0 \rangle_{\mathrm{bkg}} = 0$ by fermion parity conservation, the slope $\mathrm{d}\Delta E_\Sigma/\mathrm{d}\mu = \langle \nu_z \rangle_{\mathrm{vrtx}} - \langle \nu_z \rangle_{\mathrm{bkg}}$ yields twice the total charge. The computed slope of ~ -0.50 confirms the total charge of $-0.25e$.